

# Investigate the Effect of the Magnetic Field on the Mechanical Properties of Silicone Rubber-Based Anisotropic Magnetorheological Elastomer during Curing Process

Tao Li<sup>1,2</sup>, Ali Abd El-Aty<sup>1,2,4</sup>, Cheng Cheng<sup>1,2</sup>, Yizhou Shen<sup>1,2</sup>, Cong Wu<sup>1,2</sup>, Qiucheng Yang<sup>1,2</sup>, Shenghan Hu<sup>1,2</sup>, Yong Xu<sup>3</sup>, Jie Tao<sup>1,2,\*</sup> and Xunzhong Guo<sup>1,2,\*</sup>

<sup>1</sup>College of Material Science and Technology, Nanjing University of Aeronautics and Astronautics, Nanjing, 211100, China

<sup>2</sup>Jiangsu Key Laboratory of Advanced Structural Materials and Application, Nanjing, 211100, China

<sup>3</sup>Institute of Metal Research, Chinese Academy of Sciences, Shenyang, 110016, China

<sup>4</sup>Mechanical Engineering Department, Faculty of Engineering-Helwan, Helwan University, Cairo, Egypt

\*Corresponding Authors: Jie Tao. Email: taojie@nuaa.edu.cn; Xunzhong Guo. Email: guoxunzhong@nuaa.edu.cn

Received: 18 July 2020; Accepted: 19 August 2020

**Abstract:** In this investigation, a new silicone rubber-based MRE material was prepared to be used as a forming medium in manufacturing thin-walled complex-shaped Ni-based tubes through the bulging process. Thus, it is significant to investigate the effect of magnetic field intensity, magnetic field loading time, and angle on the mechanical properties of the prepared MRE material during the curing process. The obtained results showed that increasing the magnetic field intensity during the curing process can improve the orientation of the chain structure in the elastomer matrix effectively. However, its mechanical properties are the best under the corresponding magnetic field intensity of 321 mT. Besides, by extending the magnetic field loading time in the curing process, the orientation of the chain structure was optimized, at the same time, the mechanical properties were also improved, and the best loading time is about 20–25 min. By changing the loading angle of the magnetic field during the curing process, the mechanical properties of the MRE were improved. When the loading angle of the magnetic field is 90°, the elastomer showed the best compression mechanical properties and excellent compression reversibility. Besides, for the anisotropic MRE material, the performance with magnetic compression is always better than that without magnetic compression.

**Keywords:** Magnetorheological Elastomer (MRE); magnetic field; curing process; compression mechanical properties; chain structure

## 1 Introduction

Magnetorheological (MR) materials are new smart materials in which the magnetic field can control their mechanical properties. Due to its unique MR-effect, fast response, good reversibility (after removing the magnetic field, it can return to the original state). Besides, the mechanical properties of MR material can change continuously with the change of the external magnetic field. Thus, in recent years it gains too much attention in the applications of aerospace, automobile, architecture, and vibration control [1,2]. The



This work is licensed under a Creative Commons Attribution 4.0 International License, which permits unrestricted use, distribution, and reproduction in any medium, provided the original work is properly cited.

addition-cure silicone rubber is one of the most critical silicone products [3]. Its composition generally includes a vinyl base polymer, reinforcing material, hydrogen crosslinking agent, catalyst, inhibitor, etc. [4–6]. The vulcanization can be obtained by mixing all the raw materials and curing under certain conditions. Silicone rubber is a semi-inorganic and semi-organic polymer with Si-O-Si inorganic structure as the main chain and organic group as the side chain. It has both the properties of organic and inorganic compounds and excellent performance [7–10].

Magnetorheological Elastomer (MRE) is one of the MR materials used widely in the current few years. The micro-scale magnetic particles are added to the polymer matrix to mix and solidify under the magnetic field environment; thus, the magnetic particles in the matrix form a chain or column-like ordered structure [11,12]. MRE can address the issues of the problems of magnetic particles in MR fluid, such as easy leakage, easy settlement, environmental pollution, and poor overall stability. Besides, it does not need special containers to store [13–15]. Therefore, in the recent few years, MRE has a wide range of application prospects in the field of vibration control, such as automobile damping, building vibration isolation, anti-impact devices [15]. There are several parameters to measure the performance of MRE, such as magnetostrictive modulus, tensile strength, hardness, lagging heat generation, etc. The key parameter is the magnetostrictive modulus part of MRE, which reflects the influence of the magnetic field on the material properties and is manifested in the material properties under the coupling field of force and magnetism [16,17].

The magnetostrictive modulus of MRE is generally in a small controllable range, which hinders its industrial application [17]. The mechanical and physical properties of MRE depend on the number and size of the magnetic particles, the compatibility between polymer and magnetic particles, and the interface interaction [18]. For instance, Boczkowska et al. [18] studied the polyurethane magnetorheological elastomer composed of carbonyl iron powder with a volume fraction of 11.5% and an average particle size of 1–70  $\mu\text{m}$ . Their results showed that the rigidity of the magnetorheological elastic element could be improved by optimizing the size, the shape, and the arrangement of the particles. Winger et al. [19] compared the MR-effects of four kinds of iron particles MRE with different particle sizes using laser diffraction and X-ray microscopy. Their results showed that the MR-effect depends on the particle size fraction. Yao et al. [20] used an innovative synthetic approach to prepare a kind of magnet-induced aligning magnetorheological elastomer (MIMRE) based on the ultra-soft polymeric matrix, which makes the magnetic particles move and orientation in the elastomer matrix under the action of room temperature magnetic field. Kukla et al. [21] introduced their research results of MRE in the compression state and the effect of the magneto-static field. They introduced the attempt to describe magnetorheological with a rheological model. Metsch et al. [22] investigated the magnetostriction phenomenon of MRE using the continuum method (considering the constitutive and geometric characteristics on the micro-scale) to predict the behavior of composite materials by the homogenization method. From the perspective of macro magnetostriction, their research results are in good agreement with the existing experimental and theoretical results. Bica [23] studied the preparation process of anisotropic magnetorheological elastomer (MREs) based on silicon rubber and nano iron-based anisotropic MRE. By using the approximation of magnetic dipole moment and the ideal elastomer model, the tensions, the deformations field, and the elastic module of MREs function of magnetic field intensity were determined at magnetic field values up to 1000 kA/m. Zhang et al. [24] established a Gaussian distribution model of the field-induced properties of anisotropic MRE. The results obtained from their investigation showed the reliability of their improvement in predicting the behavior of magnetorheological elastomers accurately. Guan et al. [25] investigated the magnetostriction of MRE with carbonyl iron particles based on silicone rubber. They proposed the mechanism of the MR-effect of composite materials to explain this phenomenon. Chen et al. [26] prepared several MRE samples with different carbon black mass fractions under a constant magnetic field. Their experimental results showed that carbon black plays a vital role in improving the mechanical properties of MRE [26].

Based on the aforementioned discussion, a new silicone rubber-based MRE material was prepared in this study to be used as a forming medium in manufacturing thin-walled complex-shaped Ni-based tubes through the bulging process. Thus, it is significant to investigate the effect of magnetic field intensity, magnetic field loading time, and angle on the mechanical properties of the prepared MRE material during the curing process.

## 2 Material Description and Experimental Procedures

### 2.1 Material Description

In this study, the addition cure silicon rubber of AS40 provided by easy composites brand was selected as the matrix material to prepare the MRE material as depicted in Fig. 1.

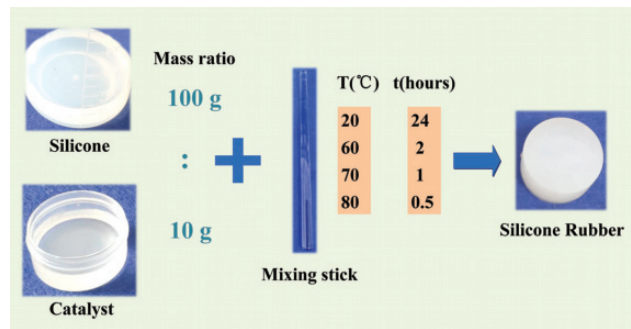


**Figure 1:** The use instructions of AS40 addition cure silicone

The selected magnetic particles in this investigation are carbonyl iron powder of MPS-MRF-15 produced by Jiangsu Tianyi ultrafine metal powder Co., Ltd., as listed in Tab. 1. The observation diagram of SEM is shown in Fig. 2. To improve the movement ability of carbonyl iron powder in the matrix material during the curing process of MRE, dimethyl silicone oil was added to the rubber in this experiment. The main function of this oil is to coat the surface of carbonyl iron particles so that it can move along the direction of the magnetic induction line under the effect of external magnetic force, which leads to form a regular chain structure.

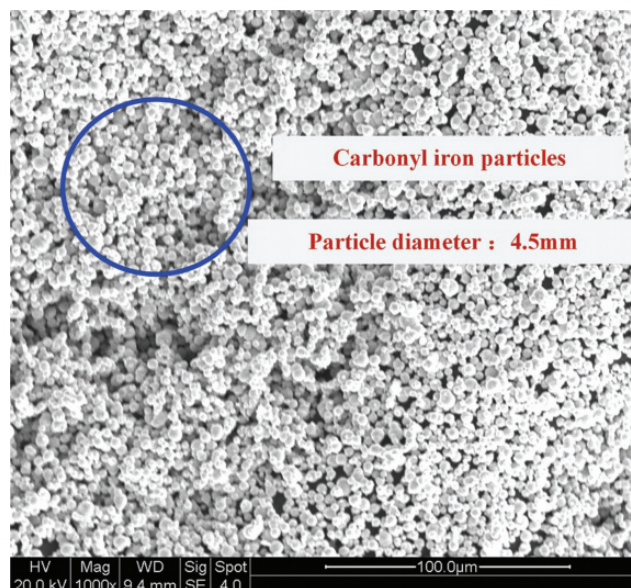


**Figure 2:** SEM morphology of carbonyl iron particles

**Table 1:** Performance parameters of MPS-MRF-15 carbonyl iron powder

Performance	Units	Value
Average particle diameter	$\mu\text{m}$	4.5
Compacted density	$\text{g}/\text{cm}^3$	4.24
Particle size distribution (D50)	$\mu\text{m}$	5.108

## 2.2 Experimental Procedures

### 2.2.1 Magnetic Field Generator

In the curing process of the magnetorheological elastomer and the subsequent testing of the elastic physical properties to reflect the magnetorheological elastomer's sensitivity to the magnetic force, it is crucial to apply the magnetic field to the experimental environment by adding an external magnetic field generator. The magnetic field generator involved in this study is depicted in Fig. 3. This device is composed of two parts: electromagnet and high-precision DC excitation source supply. The magnetic field generator can provide 600–700 mT magnetic field intensity by adjusting the external current and air gap under the experimental conditions.

**Figure 3:** Magnetic field generator: (a) Electromagnet, (b) High precision DC excitation source

### 2.2.2 Test Methods

To perform the compression experiment under a specific magnetic field condition, a magnetic field generating device was added on the testing machine, as shown in Fig. 4. Since the upper and lower pressing head of the material testing machine are magnetic conducting metals, nylon pads were added to the experimental device as a transition to prevent them from affecting the accuracy of the mechanical test results under the action of the magnetic field and eliminate the impact of the pressing head.

In the curing process, carbonyl iron powder forms a chain structure under the action of the magnetic field. To study the difference of chain structure under different magnetic field conditions, the distribution of carbonyl iron particles in magnetorheological elastomer was observed by SEM. The magnetic field conditions mainly include three aspects: magnetic field intensity, magnetic field loading time, and magnetic field loading angle. During the experiment, the composition of MRE kept constant. Firstly, silicon and catalyst were added respectively in the mass ratio of 100:10 and stirred evenly. Afterward, dimethyl silicone oil with a mass fraction of 25% was added. After stirring evenly, carbonyl iron powder with a mass fraction of 50% was added for full stirring. After completing the aforementioned steps, the liquid MR mixture was poured into the mold, and placed on the heat transfer stage that has been preheated to 70°C for curing. At the same time, the magnetic field under different conditions is loaded around it, as shown in Fig. 5. Tab. 2 introduced the experimental variables set for three magnetic field conditions in this study.

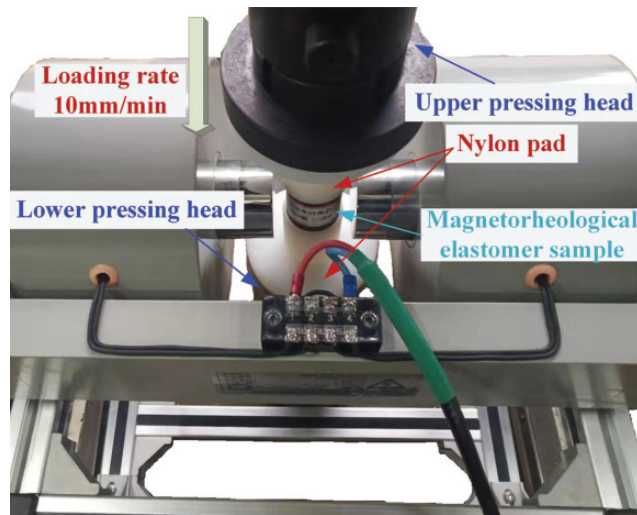


**Figure 4:** Quasi-static uniaxial compression test environment of MRE

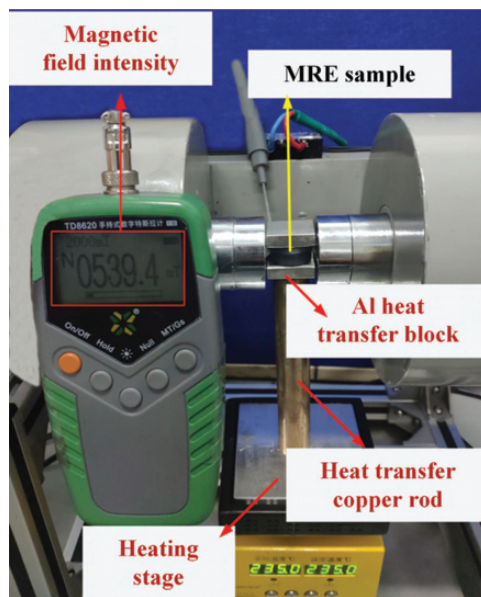


**Figure 5:** Curing environment of magnetorheological elastomer

**Table 2:** Experimental parameter settings

Conditions	Units	Value				
Magnetic field intensity (B)	mT	0	160	321	485	650
Loading time (t)	min	10	15	20	25	30
Loading angle ( $\varphi$ )	$^{\circ}$	0		45		90

### 3 Results and Discussion

#### 3.1 Influence of Magnetic Field Intensity on the Properties of MRE in the Curing Process

To investigate the influence of different magnetic field intensity on the distribution of carbonyl iron particles in MRE, five MRE samples were prepared with the magnetic field intensity of 0 mT, 160 mT, 321 mT, 485 mT and 650 mT as variables. During the preparation process, to maintain the controllability of the variables, the air gap of the magnetic field generator is kept constant at 30 mm, and the corresponding unique magnetic field intensity under the current was generated by adjusting the current intensity. SEM analysis was carried out on the prepared MRE samples under the aforementioned experimental conditions, as illustrated in Fig. 6. It is noticed from Fig. 6 that in case of applying zero external magnetic fields, the magnetic particles in the elastomer are evenly distributed, and the elastomer is isotropic as a whole. On the other hand, when the magnetic field intensity was gradually increased, the chain structure distribution of magnetic particles in the magnetorheological elastomer was gradually clear, and dimethyl silicone oil provides excellent support for the movement of magnetic particles. At this time, the elastomer is an anisotropic state.

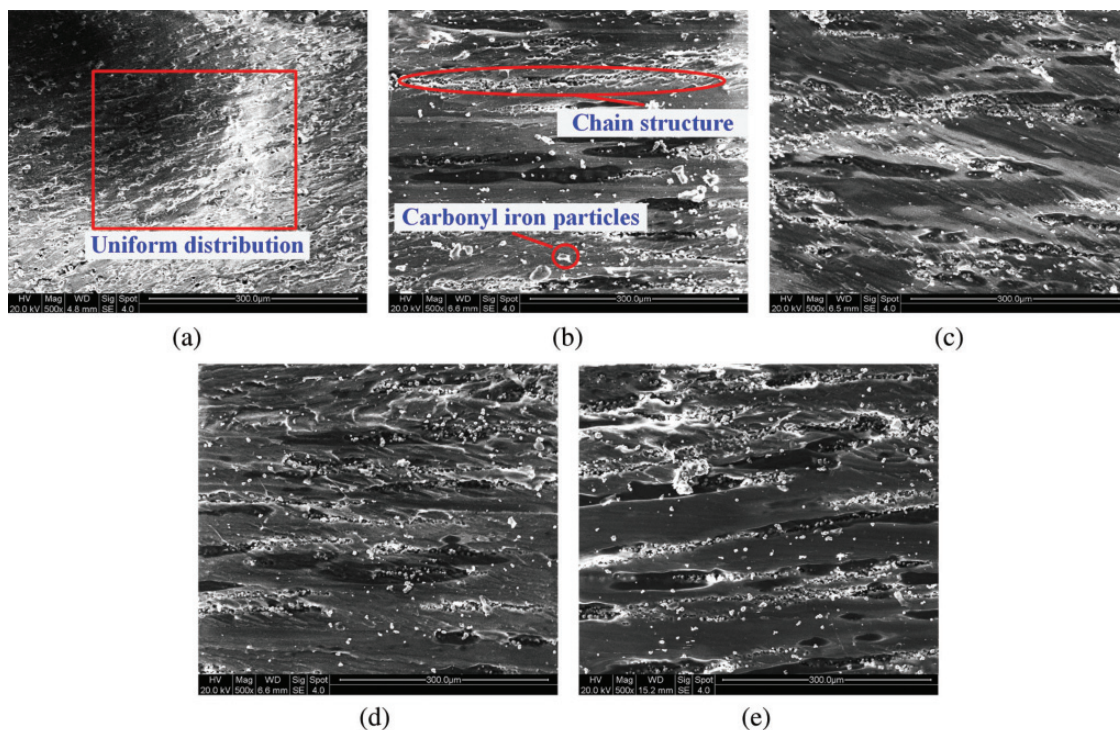


**Figure 6:** SEM observation of MRE samples under different magnetic field intensities (a) 0 mT; (b) 160 mT; (c) 321 mT; (d) 485 mT; (e) 650 mT

As shown in Fig. 7, the stress-strain curve of the MRE sample after non-magnetic compression was obtained when the magnetic field intensity and the time of the curing process are 650 mT and 30 min, respectively. The curve was divided into two parts: the elastic stage and the hyperelastic stage. In the process of compression, it was assumed that the elastic sample was fully sliding and compressed uniformly. The stress-strain relationship can be predicted by the Gaussian theory as follow:

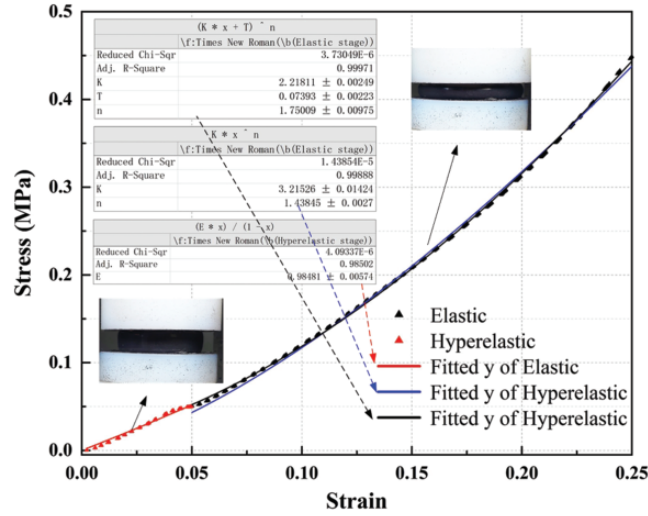


**Figure 7:** The stress-strain curve of MRE obtained by curing magnetic field intensity 650 mT and time 30 min

$$\sigma = G(\lambda^{-2} - \lambda) \tag{1}$$

where  $G$  is the shear modulus. Since rubber has a very high bulk elastic modulus, it can be regarded as incompressible for most applications, so  $E = 3G$ ;  $\lambda$  is the compression ratio,  $\lambda = 1 - \varepsilon$ , substituting  $E$  and  $\lambda$  into Eq. (1), Eq. (2) can be written as:

$$\sigma = \frac{E}{3} \left[ \frac{3\varepsilon - 3\varepsilon^2 + \varepsilon^3}{(1 - \varepsilon)^2} \right] \tag{2}$$

Under the condition of small strain, the  $\varepsilon^3$  is ignored, thus:

$$\sigma = \frac{E\varepsilon}{1 - \varepsilon} \tag{3}$$

Eq. (3) was defined as the elastic phase constitutive model shown in Fig. 7. However, it was seen from Fig. 7 that the stress-strain relationship is more in line with the power exponent relationship in the hyperelastic stage. After using the Hollomon model, it is found that the model has a significant error when the strain is close to 25%. Considering that the MRE is different from the pure rubber, the material parameter  $t$  reflecting the magnetorheological effect was introduced and refitted, and a good result is obtained.

$$\sigma = K\varepsilon + T^n \tag{4}$$

where  $K$  is the coefficient reflecting the plasticity of the material,  $T$  is the coefficient indicating the magnetorheological effect, and  $n$  is the hardening coefficient.

The stress-strain curves of MRE samples prepared under different magnetic field intensities are obtained through mechanical properties tests, as depicted in Fig. 8.

It was noticed from Fig. 8 that with the gradual increase of the magnetic field intensity during the curing process, although the chain structure orientation in the elastomer is more precise, however, the stress under the same strain does not increase in direct proportion. Under the same strain, the pre-structured MRE under 321 mT magnetic field intensity can withstand the maximum stress, followed by 160 mT and 0 mT. When the

magnetic field intensity is more than 321 mT and reaches 485 mT and 650 mT, the stress of the elastomer decreases under the same strain, which is worse than that of the elastomer sample without magnetic field (0 mT). The reason for this phenomenon is that when the magnetic field intensity increases from 0 mT to 321 mT, the magnetic field intensity increases gradually, and the magnetic particles in the elastomer also produce a certain degree of chain aggregation. While maintaining the excellent elastic modulus of the silicone rubber itself, the zero-field magnetostrictive modulus of the elastomer was also improved to a certain degree. Nevertheless, when the magnetic field intensity increases more than 321 mT and reaches 485 mT and 650 mT, the magnetic particles in the elastomer gather excessively, the number of chain structure is less, and the single-chain is thick and dense. Although this phenomenon can improve the zero-field magnetostrictive modulus of the elastomer, it has a serious damage to the elastic modulus of the silicone rubber basic body, which leads to the decline of the overall performance of the magnetorheological elastomer.

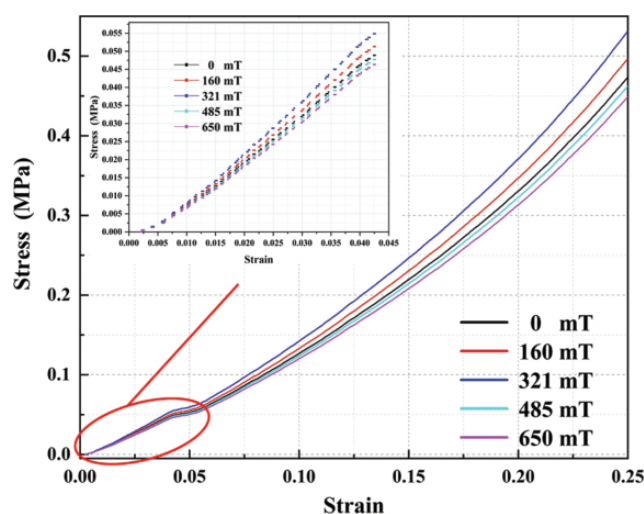


**Figure 8:** Stress-strain and constitutive curve of five samples without magnetic compression

One of the essential properties of MRE is that its mechanical properties can be changed under the action of the magnetic field. In this investigation, the stress-strain curve of MRE under the condition of magnetic compression was obtained by the compression experiment of MRE under the magnetic field intensity of 650 mT, as shown in Fig. 9. It was seen from this figure that the ordering relationship of the mechanical properties of the five samples has not changed when the magnetic field intensity of the curing process is 321 mT, the stress of MRE is still the largest, followed by 160 mT, 0 mT, 485 mT, 650 mT.

Besides, by comparing the stress of each sample under the condition of magnetic and non-magnetic, it is noticed that as long as the chain structure is formed in the elastomer, the compression performance under the condition of magnetic compression is always better than that under the condition of non-magnetic. For the elastomer prepared under the condition of non-magnetic (0 mT), due to the uniform distribution of magnetic particles in the matrix, no chain structure has been formed. Besides, its compression performance under the condition of magnetic compression is not significantly improved compared with that under the condition of non-magnetic. It was seen that the performance control advantage of anisotropic magnetorheological elastomer with the regular orientation of magnetic particles in the matrix is higher than that of isotropic elastomer.

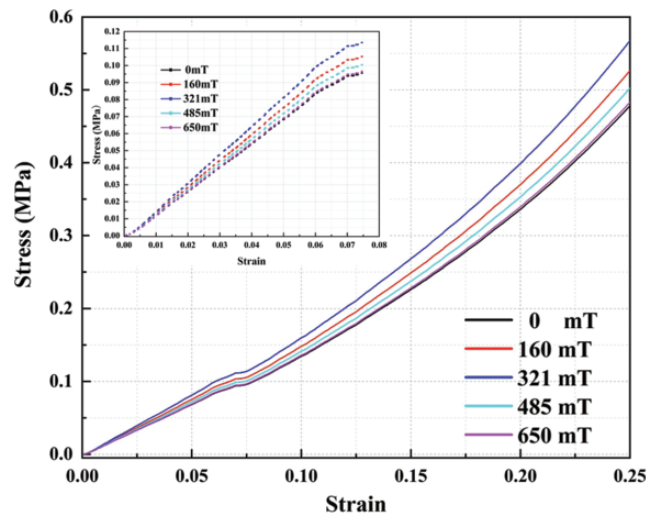


**Figure 9:** Stress strain curve of MRE (prepared at 0 mT, 160 mT, 321 mT, 485 mT, 650 mT) under magnetic (650 mT) compression

As depicted in Fig. 10, the magnetorheological effect and elastic modulus of MREs under different curing magnetic field intensity were compared. It is seen that the MR-effect and elastic modulus of the material with magnetic compression are higher than those obtained from nonmagnetic compression. Furthermore, the MR-effect can be doubled by loading the magnetic field in the compression process. In the case of magnetic compression, the increment of elastic modulus of anisotropic elastomer is significantly larger than that of isotropic elastomer. Besides, the distribution control of magnetic particles can effectively change the properties of the elastomer.

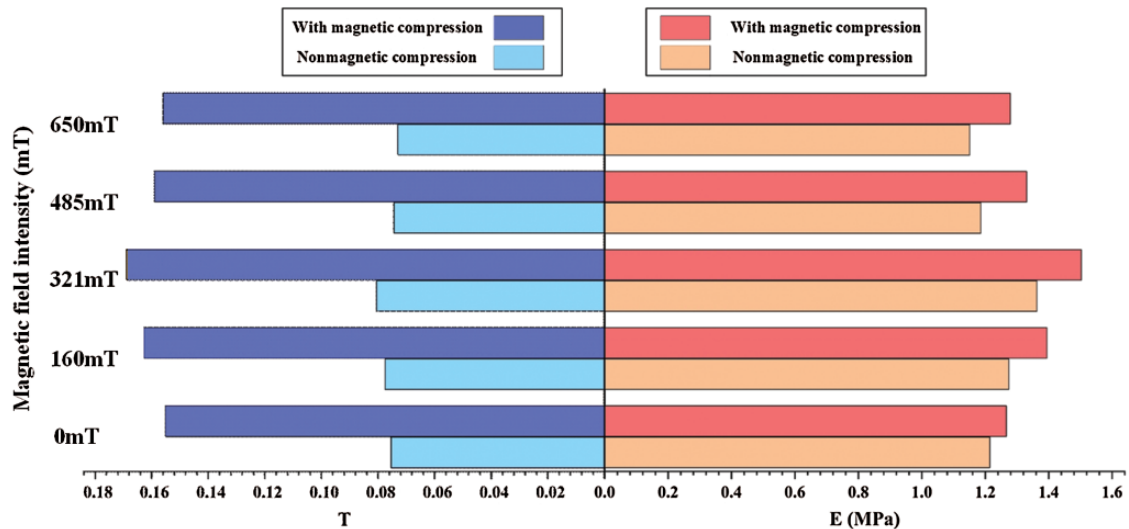


**Figure 10:** Magnetorheological effect and elastic modulus of MREs with different curing magnetic field strength

### 3.2 Impact of Magnetic Field Loading Time on the Mechanical Properties of MRE in the Curing Process

In this investigation, the impact of magnetic field loading time on the properties of MRE samples was discussed under the conditions of magnetic field loading time of 10 min, 15 min, 20 min, 25 min, and 30 min, respectively. After SEM analysis, the morphologies were obtained, as shown in Fig. 11.

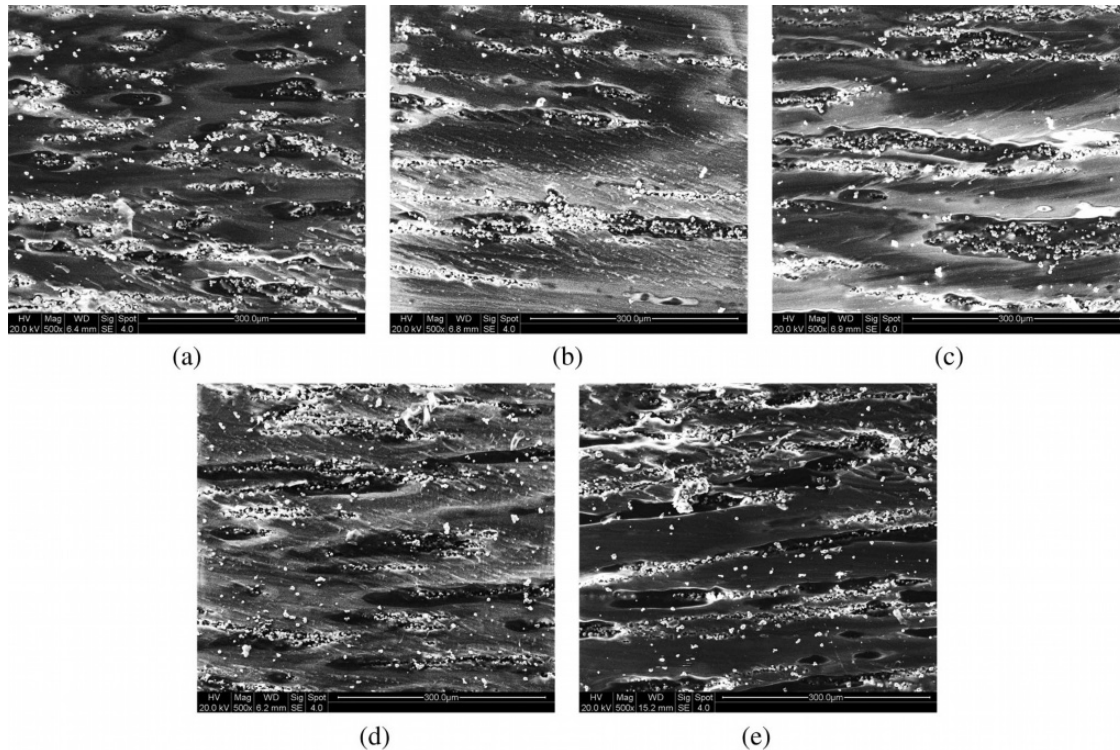


**Figure 11:** SEM morphologies of the elastomer under different magnetic field loading time (a) 10 min; (b) 15 min; (c) 20 min; (d) 25 min; (e) 30 min

According to Fig. 11, the orientation of the chain structure in the elastomer is more prominent, in which the magnetic field loading time increased from 10 min to 30 min. Among them, when the loading time is 25 min and 30 min, the orientation degree of the chain structure is slightly different. The reason is that under this curing condition, at 25 min, the liquid elastomer mixture has tended to solidify gradually, and the relative position of the magnetic particles in the elastomer has tended to be fixed. Thus, when the loading time is extended to 30 min, the chain structure showed no greater difference.

The stress-strain curves of MRE samples under different magnetic loading times were obtained by compression test under the condition of no magnetic, as depicted in Fig. 12.

According to Fig. 12, with the increase of magnetic field loading time, the stress of elastomer under the same strain condition increased gradually. Notwithstanding, when the loading time reaches 20 min, 25 min, and 30 min, the increment of the stress decreased, which is in good agreement with the morphologies obtained from SEM analysis. This is attributed to when the loading time exceeds 20 min, the chain structure in the elastomer has formed, and the elastomer itself is close to the curing state at this time, the movement ability of magnetic particles in the rubber matrix becomes slower.

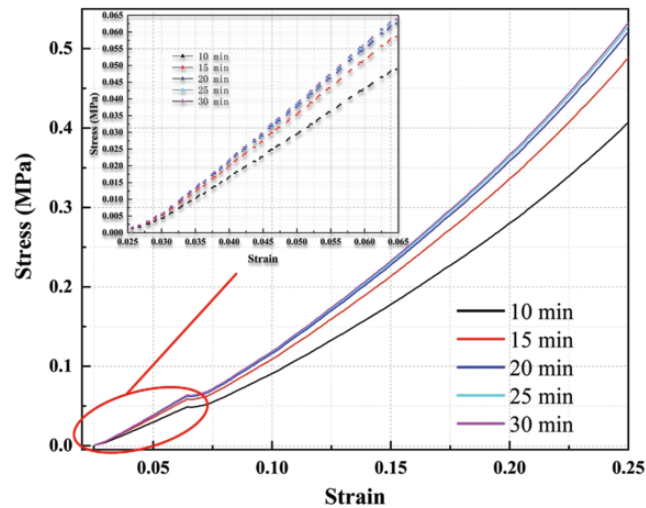


**Figure 12:** Stress-strain curves of samples under different magnetic loading times without magnetic compression

The stress-strain curves of the samples under different magnetic loading time are obtained by the compression test of the above elastomer under the condition of the magnetic field (650 mT), as depicted in Fig. 13. It is noticed from this figure that the elastic stage of the above-mentioned elastomers becomes longer when they are compressed under the magnetic condition. Compared with the previous linear deformation stage, when the strain is about 5%, the linear deformation stage under this test increases to the position where the strain is about 7.5%.

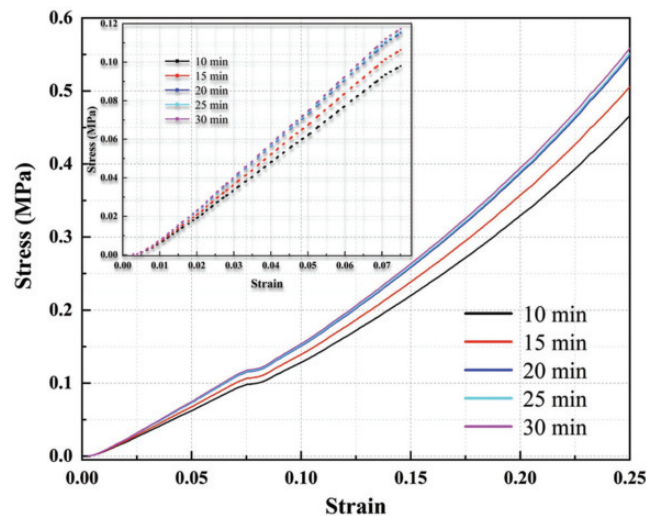


**Figure 13:** Stress-strain curves of samples under different magnetic loading times with magnetic (650 mT) compression

As shown in Fig. 14, it is noticed that the variation law of magnetorheological effect and elastic modulus is the same as that of the stress-strain curve. Besides, for observing the change rule of elastic modulus, it is also found that when the magnetic field loading time is 10 min and 15 min, the amplitude of the magnetic compression elastic modulus is small. On the other hand, when the loading time is more than 20 min, the increase of the magnetic compression elastic modulus becomes larger.

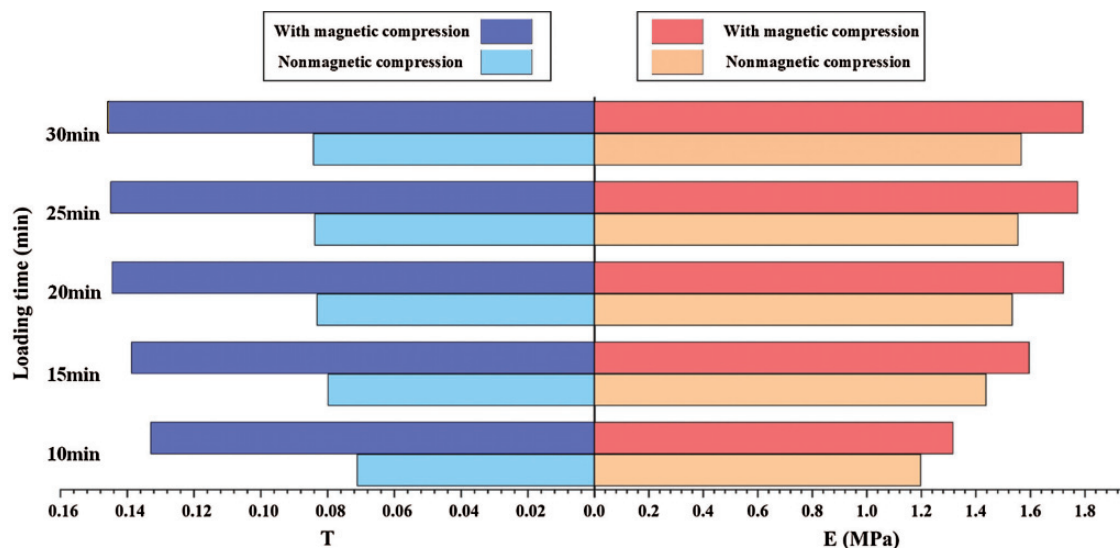


**Figure 14:** Magnetorheological effect and elastic modulus of MREs with different curing magnetic field loading time

### 3.3 Effect of Magnetic Field Loading Angle on the Properties of MRE in the Process of Pre Structure

As shown in Fig. 15, to study the influence of the magnetic field loading angle on the properties of MRE, three kinds of Al heat transfer blocks were designed and manufactured in this experiment, namely  $0^\circ$ ,  $45^\circ$ , and  $90^\circ$ .

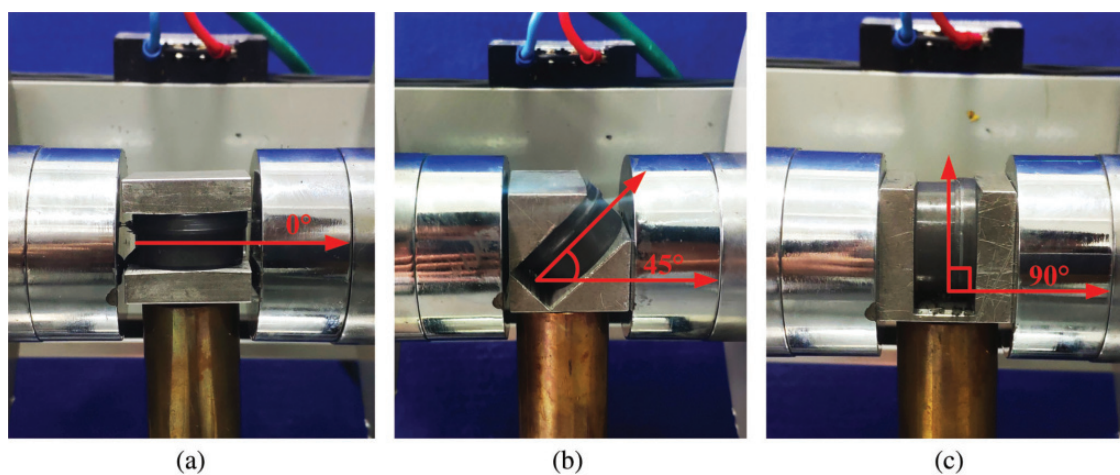


**Figure 15:** Preparation method of MRE with different magnetic field loading angles (a)  $0^\circ$ ; (b)  $45^\circ$ ; (c)  $90^\circ$

Three kinds of magnetorheological elastomers with different magnetic loading angles were prepared by the above method, and their SEM micrographs were observed, as shown in Fig. 16. It is noticed that different magnetic field loading angles have obvious effects on the formation of chain structure orientation of different angles, which makes the magnetorheological elastomers show more abundant anisotropic properties.

The compression stress-strain curves of MRE under different loading angles are obtained by compression experiments under the condition of no magnetism, as shown in Fig. 17.

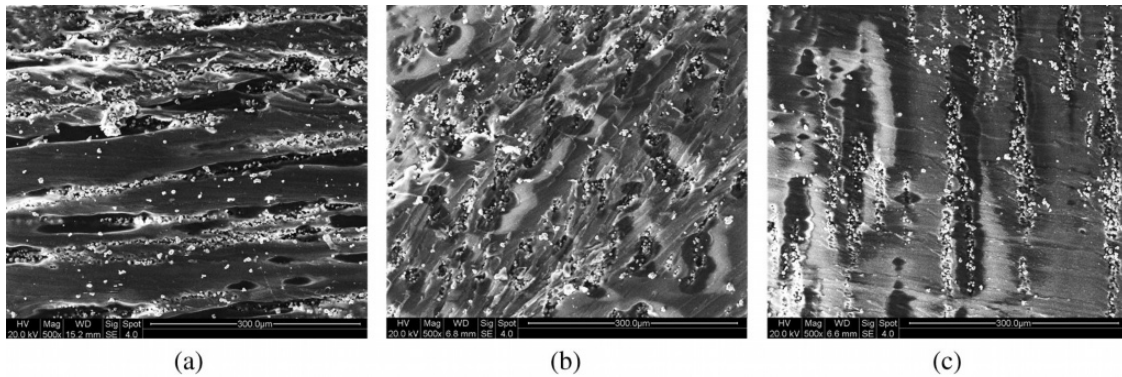


**Figure 16:** SEM morphologies of the elastomer under different magnetic field loading angles (a)  $0^\circ$ ; (b)  $45^\circ$ ; (c)  $90^\circ$

It is noticed from Fig. 17 that as the loading angle of the curing magnetic field changes from  $0^\circ$  to  $45^\circ$  to  $90^\circ$ , the stress limit of the elastomer under the same strain condition is significantly increased. When the magnetic field loading angle is  $90^\circ$ , the stress of the elastomer reaches the maximum, especially in the elastic stage, where the elastic modulus was significantly improved. On the other hand, there are some serrations in the curve at this stage appeared, which means that there is an inevitable fluctuation in the increase of stress during the gradual increase of strain. This attributed to the initial compression process, where the magnetic particles in the chain structure are gradually compressed and relatively dislocated under the action of the small compression force of the elastomer. When the adjacent magnetic particles contact with each other, the overall stress of the elastomer increased. Besides, when the adjacent magnetic particles are relatively dislocated, the overall stress of the elastomer decreased. This process is repeated in the linear deformation stage, resulting in the zigzag phenomenon depicted in Fig. 17.

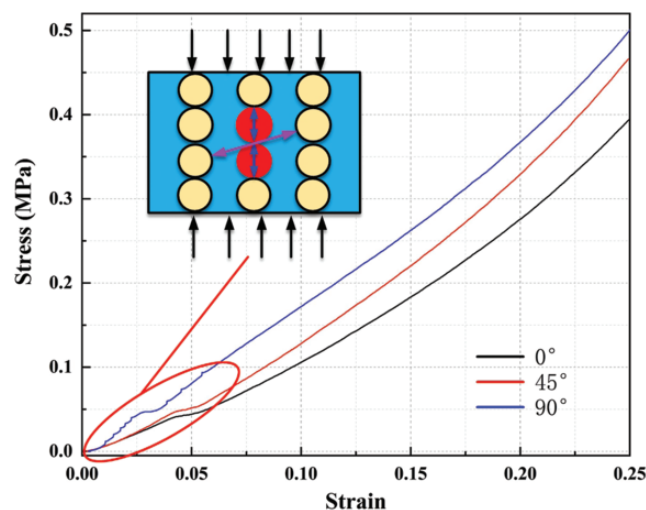


**Figure 17:** The Stress-strain curves of samples with different magnetic loading angles under the condition of no magnetic compression

The stress-strain curve of the prepared MRE samples mentioned above under different magnetic loading angles is shown in Fig. 18 after compression under magnetic (650 mT) conditions. It is noticed from the figure that when the curing magnetic field loading angle is  $90^\circ$ , the elastomer bears the maximum stress. Besides, compared with the non-magnetic compression, the stress-bearing limit of each elastomer under magnetic compression was also improved.

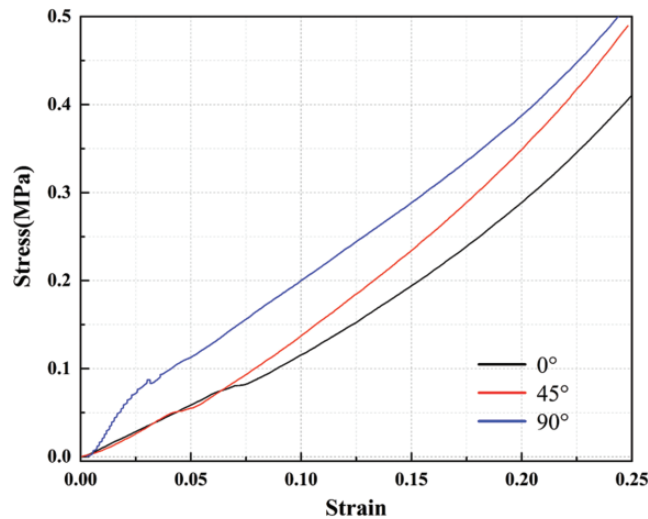


**Figure 18:** The stress-strain curves of samples with different magnetic loading angles under the condition of magnetic compression

As shown in Fig. 19, the magnetorheological effect and elastic modulus of magnetorheological elastomer were affected by changing the magnetic loading angle during the pre-structure process. When the magnetic field loading angle is  $90^\circ$ , the elastic modulus of the elastomer increases significantly, and the increment is nearly double.

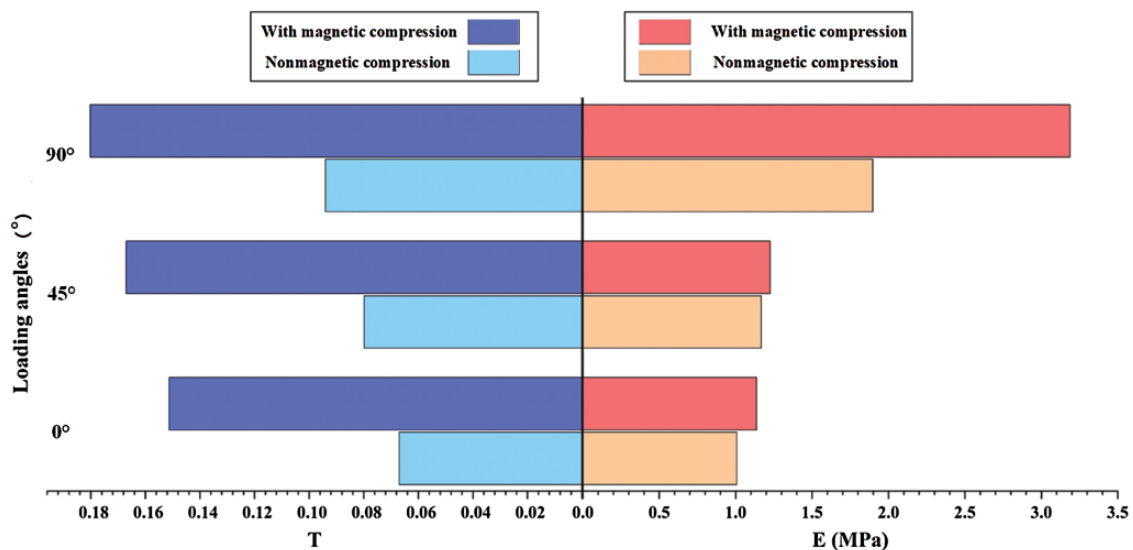


**Figure 19:** The Magnetorheological effect and elastic modulus of MREs with different curing magnetic field loading angles

As a kind of reversible functional material, the key to the reversibility of MRE is whether the chain structure of magnetic particles is destroyed under the condition of large strain. In this investigation, the morphologies of MRE with and without magnetic compression under different magnetic loading angles were observed by SEM. As depicted in Fig. 20, it is observed that the chain structure orientation of MRE after compression is still clear, and the compression force has no effect on its structure. Therefore, the elastomer based on this method is used for the bulging of complex curved components. Its compression performance and reversibility are reliable.

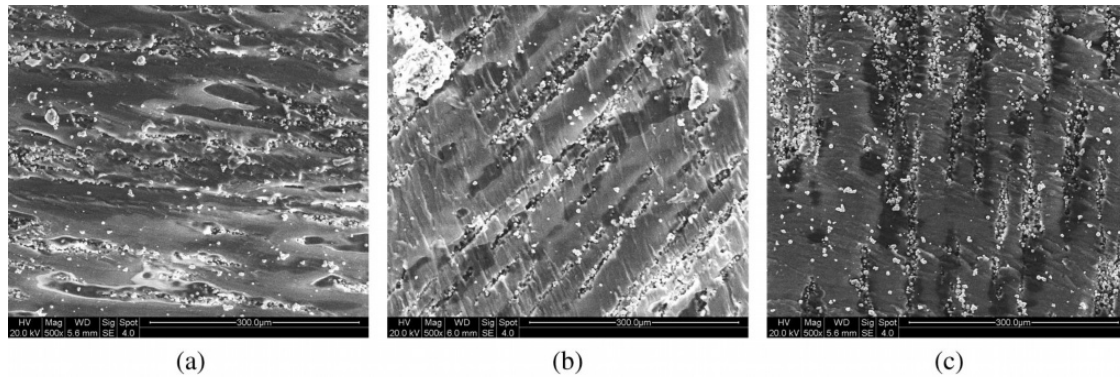


**Figure 20:** The SEM morphologies of samples with different magnetic loading angles after the compression test

#### 4 Conclusion

In this investigation, the mechanical properties and morphologies of anisotropic MRE with silicone rubber as matrix and carbonyl iron powder as magnetic particles under different magnetic fields were studied. According to the obtained results, the main conclusions can be deduced as follows:

- (1) There are two parts in the stress-strain constitutive relation of the magnetorheological elastomer-based on silicone rubber in the compression test. The first part is the elastic stage in which the constitutive relation conforms to  $\sigma = E\varepsilon/(1 - \varepsilon)$ ; the second part is the hyperelastic stage in which the constitutive relation conforms to  $\sigma = K\varepsilon + T^n$ .
- (2) In the process of elastomer preparation, with the increase of the magnetic field intensity, the chain structure orientation of the magnetic particles in the matrix is gradually clear, and the material is anisotropic. Its compression performance exhibits the best state when the magnetic field intensity of sample preparation is 321 mT, and when the magnetic field intensity reaches 485 mT and 650 mT, its compression performance decreases. Besides, when there is magnetic compression, it can improve the mechanical properties of anisotropic MRE.
- (3) With the increase of the magnetic field loading time in the preparation process, the chain structure orientation of the elastomer becomes more apparent, and its compression performance gradually increased with the increase of the time. The best loading time is 20–25 min, and the magnetic compression performance is better than the non-magnetic compression.
- (4) With the change of the magnetic field loading angle during the preparation of the elastomer, the chain structure in the elastomer matrix also presents the corresponding angle orientation. When the magnetic field loading angle of sample preparation is  $90^\circ$ , the compression performance of the elastomer is the best. At the same time, with magnetic compression, the overall performance of the elastomer can also be improved. Besides, the elastomer shows good reversibility during compression.

**Funding Statement:** The funding for the investigation in this paper mainly comes from the following funds. Funded by the National Natural Science Foundation Key Project of China (Grant No. U1937206), the authors are Li, Xu, Guo, the specific grant numbers was RMB 100,000. Funded by the Jiangsu Province Key Research and Development Project (No. BE2019007-2), the authors are Abd, Cheng, the specific grant numbers was RMB 200,000. Funded by the Opening Project of Jiangsu Key Laboratory of Advanced Structural Materials and Application Technology (No. ASMA201903), the authors are Wu, Yang, Hu, the specific grant numbers was RMB 50,000. Funded by the Basic Scientific Research Operations (Approval No. NT2020015), the authors are Shen, Tao, Guo, the specific grant numbers was RMB 100,000.

**Conflicts of Interest:** The authors declare that they have no conflicts of interest to report regarding the present study.

## References

1. Qiu, J. D., Lai, X. J., Fang, W. Z., Li, H. Q., Zeng, X. R. (2017). An efficient strategy for simultaneously improving tracking resistance and flame retardancy of addition-cure liquid silicone rubber. *Polymer Degradation and Stability*, 144, 176–186. DOI 10.1016/j.polyimdegradstab.2017.08.005.
2. Li, Y. P., Zeng, X. R., Lai, X. J., Li, H. Q., Fang, W. Z. (2017). Effect of the platinum catalyst content on the tracking and erosion resistance of addition-cure liquid silicone rubber. *Polymer Testing*, 63, 92–100. DOI 10.1016/j.polymertesting.2017.08.017.
3. Pan, K. X., Zeng, X. R., Li, H. Q., Lai, X. J. (2016). Synthesis of silane oligomers containing vinyl and epoxy group for improving the adhesion of addition-cure silicone encapsulant. *Journal of Adhesion Science and Technology*, 30(10), 1131–1142. DOI 10.1080/01694243.2016.1142806.
4. Hara, H. (2010). Addition cure silicone rubber adhesive composition and making method. U.S. Patent 7,825,177.
5. Kashiwagi, T., Shiobara, T. (2009). Silicone rubber composition, light-emitting semiconductor embedding/protecting material and light-emitting semiconductor device. U.S. Patent 7, 521,813.
6. Pan, Z. Q., Sun, R., Zhu, S. L., Kang, Y. Z., Huang, B. S. et al. (2018). The synthesis, characterization and properties of silicone adhesion promoters for addition-cure silicone rubber. *Journal of adhesion science and Technology*, 32(14), 1517–1530. DOI 10.1080/01694243.2018.1428059.
7. Higuchi, M., Matsuda, M., Ishiyama, Y., Ibaraki, K., Abe, H. (2001). Board-to-board connector capable of readily electrically connecting two parallel boards to each other. U.S. Patent 6, 312,263.
8. Bendahou, D., Bendahou, A., Seantier, B., Lebeau, B., Grohens, Y. et al. (2018). Structure-thermal conductivity tentative correlation for hybrid aerogels based on nanofibrillated cellulose-mesoporous silica nanocomposite. *Journal of Renewable Materials*, 6(3), 299–313.
9. Yang, C., Wu, Y. (2017). High-performance silicone rubber composites via non-covalent functionalization of carbon nanotubes. *Journal of Macromolecular Science, Part B*, 56(10), 790–799. DOI 10.1080/00222348.2017.1385352.
10. Liang, W. J., Ge, X., Ge, J. F., Li, T. H., Zhao, T. K. et al. (2018). Reduced graphene oxide embedded with MQ silicone resin nano-aggregates for silicone rubber composites with enhanced thermal conductivity and mechanical performance. *Polymers*, 10(11), 1254. DOI 10.3390/polym10111254.
11. Tian, T., Nakano, M. (2018). Fabrication and characterisation of anisotropic magnetorheological elastomer with 45 iron particle alignment at various silicone oil concentrations. *Journal of Intelligent Material Systems and Structures*, 29(2), 151–159. DOI 10.1177/1045389X17704071.
12. Wu, C. J., Zhang, Q. X., Fan, X. P., Song, Y. H., Zheng, Q. (2019). Smart magnetorheological elastomer peristaltic pump. *Journal of Intelligent Material Systems and Structures*, 30(7), 1084–1093. DOI 10.1177/1045389X19828825.
13. Zhang, T., Ren, Z. (2019). Design and experimental study of vibration reducing experimental device for magnetorheological elastomer. *Journal of Physics: Conference Series*, 1187(3), 032048. DOI 10.1088/1742-6596/1187/3/032048.

14. Fu, J., Li, P. D., Wang, Y., Liao, G. Y., Yu, M. (2016). Model-free fuzzy control of a magnetorheological elastomer vibration isolation system: analysis and experimental evaluation. *Smart Materials and Structures*, 25(3), 035030. DOI 10.1088/0964-1726/25/3/035030.
15. Leng, D. X., Xiao, H. Y., Sun, L., Liu, G. J., Wang, X. J. et al. (2018). Study on a magnetorheological elastomer-base device for offshore platform vibration control. *Journal of Intelligent Material Systems and Structures*, 30(2), 243–255. DOI 10.1177/1045389X18808398.
16. Chen, S. W., Li, R., Zhang, Z., Wang, X. J. (2016). Micromechanical analysis on tensile modulus of structured magneto-rheological elastomer. *Smart Materials and Structures*, 25(3), 035001. DOI 10.1088/0964-1726/25/3/035001.
17. Yu, M., Qi, S., Fu, J., Zhu, M., Chen, D. (2017). Understanding the reinforcing behaviors of polyaniline-modified carbonyl iron particles in magnetorheological elastomer based on polyurethane/epoxy resin IPNs matrix. *Composites Science and Technology*, 139, 36–46. DOI 10.1016/j.compscitech.2016.12.010.
18. Boczkowska, A., Awietjan, S. F., Pietrzko, S., Kurzydłowski, K. J. (2012). Mechanical properties of magnetorheological elastomers under shear deformation. *Composites Part B: Engineering*, 43(2), 636–640. DOI 10.1016/j.compositesb.2011.08.026.
19. Winger, J., Schumann, M., Kupka, A., Odenbach, S. (2019). Influence of the particle size on the magnetorheological effect of magnetorheological elastomers. *Journal of Magnetism and Magnetic Materials*, 481, 176–182. DOI 10.1016/j.jmmm.2019.03.027.
20. Yao, J. R., Sun, Y. Y., Wang, Y., Fu, Q., Xiong, Z. Y. et al. (2018). Magnet-induced aligning magnetorheological elastomer based on ultra-soft matrix. *Composites Science and Technology*, 162, 170–179. DOI 10.1016/j.compscitech.2018.04.036.
21. Kukla, M., Górecki, J., Malujda, I., Talaśka, K., Tarkowski, P. (2017). The determination of mechanical properties of magnetorheological elastomers (MREs). *Procedia Engineering*, 177, 324–330. DOI 10.1016/j.proeng.2017.02.233.
22. Metsch, P., Kalina, K. A., Spieler, C., Kästner, M. (2016). A numerical study on magnetostrictive phenomena in magnetorheological elastomers. *Computational Materials Science*, 124, 364–374. DOI 10.1016/j.commatsci.2016.08.012.
23. Bica, I. (2012). The influence of the magnetic field on the elastic properties of anisotropic magnetorheological elastomers. *Journal of Industrial and Engineering Chemistry*, 18(5), 1666–1669. DOI 10.1016/j.jiec.2012.03.006.
24. Zhang, W., Gong, X. L., Chen, L. (2010). A Gaussian distribution model of anisotropic magnetorheological elastomers. *Journal of Magnetism and Magnetic Materials*, 322(23), 3797–3801. DOI 10.1016/j.jmmm.2010.08.004.
25. Guan, X., Dong, X., Ou, J. (2008). Magnetostrictive effect of magnetorheological elastomer. *Journal of Magnetism and Magnetic Materials*, 320(3–4), 158–163. DOI 10.1016/j.jmmm.2007.05.043.
26. Chen, L., Gong, X. L., Li, W. H. (2008). Effect of carbon black on the mechanical performances of magnetorheological elastomers. *Polymer Testing*, 27(3), 340–345. DOI 10.1016/j.polymertesting.2007.12.003.